INSTITUTE OF THEORETICAL ASTROPHYSICS
BLINDERN — OSLO

REPORT No. 61

A NEW METHOD FOR MEASUREMENT OF GRANULAR VELOCITIES

By
BO NYBORG ANDERSEN

Reprosentralen
Universitetet i Oslo
Oslo 1984

INSTITUTE OF THEORETICAL ASTROPHYSICS

BLINDERN — OSLO

REPORT No. 61

A NEW METHOD FOR MEASUREMENT OF GRANULAR VELOCITIES

By

BO NYBORG ANDERSEN

Reprosentralen

Universitetet I Oslo

Oslo 1984

Summary: A new, supplementary method to measure granular velocities is presented. The method utilizes the Doppler shift caused by the line of sight component of the solar rotation to cause a wavelength shift through spectral lines as function of heliocentric angle. By measuring the center-to-limb variation of the granular intensity fluctuations at different wavelength positions in the lines, the velocities are found. To do this, assumptions regarding the geometrical structure of the velocity and intensity fields have to be made. Preliminary application of the method results in a steep velocity gradient suggesting zero velocity at a height of 200 km above $\tau_{500} = 1$. Possible causes are discussed.

1. Introduction

Our knowledge of physical processes like the energy transport in the solar atmosphere depends on our ability to construct accurate model atmospheres. A detailed knowledge of the convective velocities is a necessity in model construction as well as for our physical understanding of the atmosphere.

The convective velocities can in principle be measured directly from granular Doppler shifts at different heliocentric angles. Methods using contrast differences between granules and intergranular lanes as function of position in absorption lines have also been used (Bray et al. 1976 hereafter designated BLT, Beckers 1968). The dramatic change in contrast with position in the line is most clearly demonstrated in the observations presented by BLT.

Owing to the fact that the velocity changes sign over a distance (≈1 arc.-sec.) comparable to the spatial resolution of the telescopes the uncertainties for both methods are very large. When Doppler shifts are measured directly no assumptions have to be made about the velocity field. However, the method has the drawbacks of being one-dimensional and generally only including a few (< 100) granules.

In order to apply the "tuned filtergram method" a high correlation between intensity and velocity is required (Leigthon et al. 1962, Beckers 1968, BLT). High correlation is here used for the situation with large cross-correlation at zero phase shift. For the convective velocities this correlation is not known with sufficient accuracy. For intermediate values of the correlation coefficient only the correlated part of the velocity/intensity field will influence the measurements. Figure 1 shows a hypotetical situation with equal Gaussian line profiles in granules and in intergranular areas. Here we have assumed that the velocities only affect the wavelength displacements of the lines. It appears that the maximum in the contrast occurs in the red wing of the average line profile.

The large uncertainties in the existing methods make it desireable to introduce independent methods for measurements of granular/convective velocities.

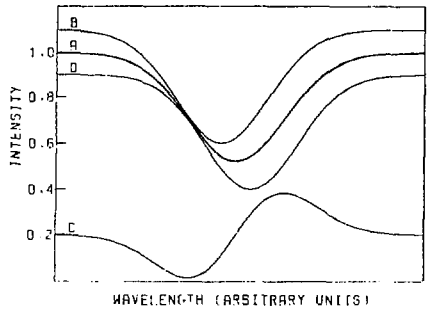

Fig.1. The simulated line profiles of a bright element (B) rising and a dark element (D) falling with velocities equivalent to 0.1 Doppler widths of the average profile respectively. The continuum contrast is 20%. The line profile (A) is an equal average of line profiles B and D. The contrast between the bright and dark profiles as function of wavelength is shown (C).

In section 2 of this paper we describe a new, supplementary method for measuring the granular convective velocities. This method makes use of the Doppler shift caused by the solar rotation to "scan" through spectral lines. By studying the variation of contrast as function of position on the Sun (i.e. also as wavelength position in the spectral lines) we can derive values for the convective velocities.

In section 3 we present the observations, discuss the velocity model and present some preliminary results for the granular convective velocities.

In section 4 we discuss some physical implications of these results and present the advantages and limitations of the method.

2.Principles of Observational Method

2.1 DESCRIPTIVE BACKGROUND

The wavelength position of a solar line is shifted with respect to a fixed laboratory wavelength due to line of sight velocities. We shall concentrate

on the lineshifts caused by solar rotation and by convective velocities. The line of sight velocity V_{LS} caused by a solar rotation may be written in units of km/s (Scherrer et al. 1980)

$$V_{LS} = (2.03 - 0.28\sin^2 B - 0.28\sin^4 B)\cdot\sin\Phi\cdot\cos B. \qquad (1)$$

Here B is the heliographical latitude and Φ the angle from the solar meridian. No evidence of short time variation of the solar rotation rate have been established. The works of Schröter et al. (1978) show that the observed variations are dominantly caused by instrumental and other terrestial effects. In addition the line of sight velocity has contributions from the orbital and rotational velocities of the Earth. The correction employed is described by Howard and Harvey (1970). Close to the solar limb the "limb effect" will cause an additional velocity component away from the observer. In this paper only data with heliocentric distances smaller than 60° are used. At these disk positions the line center limb effect for a medium strong photospheric line is less than 55 m/s (Brandt and Schröter 1982). For weaker lines and away from the line center this effect increases (Dravins et al. 1981). However, for all the line strengths and heliocentric positions used in this paper the effect is less than 200 m/s. Since the limb effect is caused by spatial averaging of the granular velocities it must clearly be smaller than these and is not taken into account in this preliminary application of the method.

When the angular resolution is better than or comparable to the sizes in the granular field, small scale intensity fluctuations are evident in one-dimensional scans across the solar disc (Figure 2). The numerical value of the center to limb variation (CLV) of the intensity fluctuations ($\Delta I_{r.m.s.}$) will depend on the wavelength and on the spatial resolution. Two scans across the solar disc carried out in the Fe I 656.9 nm line and a nearby continuum are shown in Figure 2. When a scan is carried out at a fixed wavelength within a spectral line the continuum intensity variations are superposed on the intensity variation caused by the Dopplershifted bright and dark elements in the granular field combined with the intensity gradient in the line. This effect will, as can be seen from Figure 1, depend on the position in the average line profile. This position is dependent on the line of sight velocity components of the solar rotation.

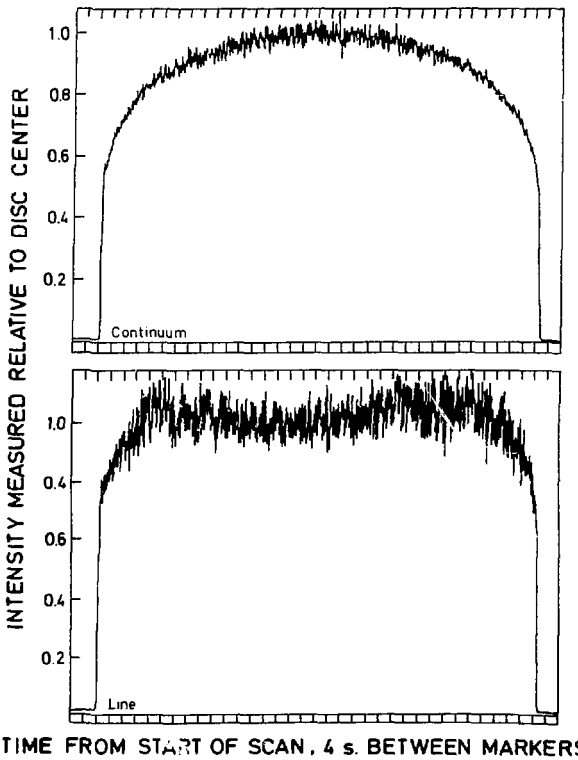

Fig.2. Simultainous equatorial drift scans across the Sun at fixed laboratory wavelengths with an entrance aperture of 1.4 arc.sec. square. The intensites have been normalized to solar disc center intensities. The upper scan was carried out with a spectral resolution of 20 pm in a continuum window near 657.5 nm. The lower scan was done with a 3 pm spectral resolution in the Fe I 656.9 nm line. The scan was carried out such that the disc center was observed in the line center.

2.2 MATHEMATICAL FORMALISM

BLT have presented a mathematical formalism that describes the variation in contrast as function of wavelength in the spectral line under the influence of spectral and angular degradation of the image. The equations presented here are mainly taken from their work or derived thereof.

The average line profile of a solar absorption line can be expressed in terms of granular (g) and intergranular (i) line profiles,

$$I_a(\Delta\lambda) = \frac{I_g(\Delta\lambda) + R \cdot I_i(\Delta\lambda)}{1 + R}, \qquad (2)$$

where R is the ratio between intergranular and granular areas. The separation between a given wavelength and the center of the average line profile is $\Delta\lambda$. Generally it is not possible to describe the whole profile of solar spectral lines by pure Gaussian profiles. But for weak lines and the cores of medium strong lines used in this work, this is a satisfactory description. Assuming Gaussian line- and instrumental profiles the spectrally degraded line profiles for the granular and intergranular areas can be written,

$$I_g(\Delta\lambda) = 1.0 - \frac{A_g}{B_g} \exp\left[-\left(\frac{\Delta\lambda - D_g}{B_g}\right)^2\right] \qquad (3)$$

and

$$I_i(\Delta\lambda) = A - \frac{A_i}{B_i} \exp\left[-\left(\frac{\Delta\lambda - D_i}{B_i}\right)^2\right] \qquad (4)$$

where,

$$D_g = \lambda \cdot v_g/c$$

$$D_i = \lambda \cdot v_i/c$$

$$A_g = (1-J_g) \cdot \Delta\lambda_g \qquad (5)$$

$$B_g = (\Delta\lambda_g^2 + b^2)^{1/2}$$

$$A_i = (A - J_i)\cdot\Delta\lambda_i$$

$$B_i = (\Delta\lambda_i^2 + b^2)^{1/2}$$

The velocities for granules and intergranular areas are designated v_g and v_i, respectively. The parameters J_g, J_i and $\Delta\lambda_g$, $\Delta\lambda_i$ refer respectively to center intensities and line widths of the unsmeared line profiles. The continuum intensity ratio between the intergranular areas and granules is A and λ is the wavelength. The parameter b describes the width of the spectral resolution of the observing instrument. The instrumental profile is given by

$$I_p(\Delta\lambda) = \frac{1}{b\sqrt{\pi}} \exp\left[-\left(\frac{\Delta\lambda}{b}\right)^2\right] \qquad (6)$$

We define the contrast between dark and bright and dark areas at a given wavelength as,

$$C'(\Delta\lambda) = \frac{I_g(\Delta\lambda)}{I_i(\Delta\lambda)} - 1.0 \ . \qquad (7)$$

The absolute value is chosen as our observational method cannot discern between positive and negative values of the contrast.

The influence of spatial degradation may be described by several methods. The more accurate methods as described by Brahde (1974) and Wittman and Mehltretter (1977) require accurate knowledge of the straylight (smearing) function. Generally this is not known to sufficient accuracy to justify these labourous methods. For simplicity we will use the straylight influenced contrast $C(\Delta\lambda)$ as derived from Gray (1976), Andersen et al. (1977), BLT and equation 7,

$$C(\Delta\lambda) = C'(\Delta\lambda)\cdot(1-S). \qquad (8)$$

Here the spatial degradation parameter S has to be determined. BLT derived

a semi-theoretical scheme to find S, we will use a purely empirical method.

The connection between the observed $\Delta I_{r.m.s.}$ and the contrast C depends on the geometry of the granular intensity distributions. From Wittman (1979, 1981) we find for a stepfunction and for a sinusodal variation, respectively

$$\Delta I_{r.m.s.} = \frac{C \cdot \sqrt{R}}{R+1+C} \quad , \tag{9a}$$

$$\Delta I_{r.m.s.} = \frac{C}{\sqrt{2}\ (C+2)} \quad . \tag{9b}$$

For values of R≈1 the inaccuracy introduced in $\Delta I_{r.m.s.}$ by the lack of knowledge of the geometrical configuration is $\sqrt{2}/2$.

We have used Equations 1 to 7 to generate a hypothetical example (Figure 3) showing the CLV of the contrast between bright, rising and dark, falling areas observed at a fixed laboratory wavelength. The wavelength shift of the average profile caused by the line of sight component of the solar rotation at three heliocentric positions is shown in the upper row of Figure 3. In this case the fixed observational wavelength was chosen such as to observe the line center at solar disc center. In the central row the individual Doppler shifted granular and intergranular line components of the average profiles are shown. The contrast between bright and dark elements as function of wavelength through the lines at three heliocentric angles is indicated in the lower row. Combining the contrast shown at the fixed wavelength for the three heliocentric angles shown in Figure 3 (i.e. -30, 0 and 30 degrees) with similar calculations for 10 other positions we get the contrast dependence of heliocentric angle shown at the bottom of Figure 3. In this example we see clearly maximum and minimum values. The positions and values of these exstrema are functions of granular velocity, intensity and line parameters. By observing the CLV of the contrast C (or $\Delta I_{r.m.s.}$ using the equations 9) we can derive information about the physical parameters of the granular intensity or velocity fields. As the fixed observational wavelength for each scan is varied the possible combinations of the free parameters (i.e. line and velocity parameters) are reduced.

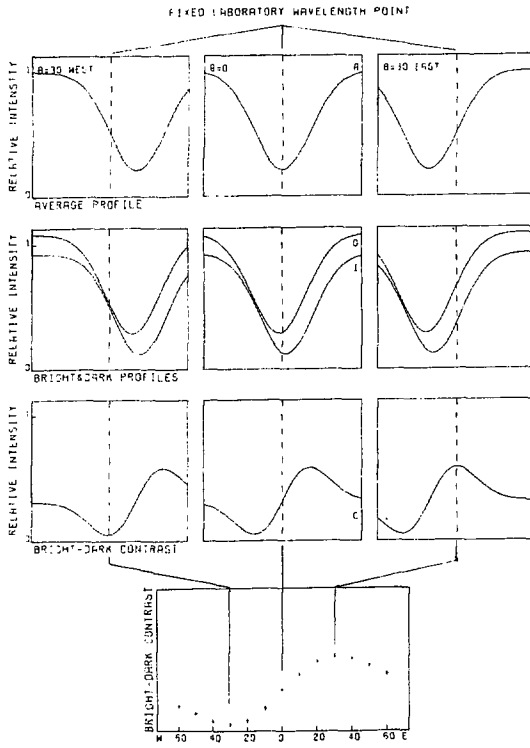

Fig.3. The upper row shows how the solar rotation causes a fixed laboratory wavelength to scan through a spatially averaged solar spectral line as function of heliocentric angle along the solar equator. In this case the fixed observation wavelength is chosen such that the disc center is observed at line center. The dotted vertical lines in the three columns give the position of the fixed observing wavelength at the heliocentric angles 30 degrees west, center and 30 degrees east respectively. The middle row indicates the granular (G) and intergranular (I) line components of the average profile. The lower row shows how the contrast between granules and intergranular areas varies as function of wavelength through the average spectral line profile. At the bottom is shown how the granule/intergranular contrast will vary as function of heliocentric angle. It is indicated where the spectral line examples are positioned in angle.

3. Preliminary Application of the Method

3.1 INSTRUMENTATION

The solar tower and the large horizontal spectrograph at the Oslo Solar Observatory were used for the observations. The tower telescope has a primary mirror with focal length 29.5 meters and an aperture of 0.35 m. More details are described by Brahde (1967). The spectrograph is of the Czerny-Turner type with 14 m focal lengths of collimator and camera mirrors. The grating has 630 lines/mm and an effective area of 150 x 250 mm^2. The signals were recorded photoelectrically by two EMI 9698B photomultiplier tubes. One of these (channel 1) is mounted on a sled driven by a computer controlled stepmotor, each step is 15μm. The other tube (channel 2) is positioned manually on the redward side of Channel 1. The data are digitized by a 10-bit AD-converter and written continously on a 9-track magnetic tape by a Hewlett-Packard 2100A minicomputer. Detailed descriptions of the spectrograph and register equipment are given by Andersen (1981). The software for the computer control of the spectrograph and the observations are described by Andersen (1979) and Marstad (1981).

3.2 CHOICE OF SPECTRAL LINES

In order to apply the present method it is necessary to have detailed knowledge of the line profiles in granules and in intergranular areas (the wavelength positions will be determined by the method). Possible height resolution is achieved by using the effective heigth of line formation as described by several authors (Beckers and Milkey 1975, Altrock et al. 1975).

Only iron lines were selected because of the large abundance of varying line strengths in the solar spectrum, the availability of laboratory measurements of oscillator strengths and the lack of hyperfine-structure. Four relatively unblended lines were selected, in addition Fe 656.9 nm was used. Although this line has strong water vapour blends it has been used extensively in earlier contrast measurements of granular velocities (Beckers 1968, BLT). The atomic and empirical data for lines and average line profiles are given in Table 1. The oscillator strengths are from

Baschek (1963) and May et al. (1978), other data are from Moore et al. (1966) and Andersen (1981).

For each line the LTE line profile at several heliocentric angles in the HSRA (Gingerich et al. 1971) model atmosphere were calculated. For all lines except 557.6 nm a fit to the observed profile within 0.5% was achieved. As pointed out by Altrock et al. (1975) the assumption of LTE breaks down in the core of this line. The close fit was made possible by a macro/micro-turbulence that decreases with heigth. The average velocity model for best fit was close to that of Hollweger and Müller (1974).

Table I. Average Line Parameters

Line (pm)	Center Intensity	Eq.Width (pm)	FWHM (pm)	Ex. pot. (eV)	Log gf.
Fe I 557.6	0.198	12.5	12.25	3.43	- 0.6
Fe I 633.0	0.685	3.6	9.53	4.73	- 1.12
Fe II 643.2	0.623	4.3	10.54	2.89	- 3.6
Fe I 656.9	0.401	7.3	11.09	4.73	- 0.6
Fe I 659.3	0.309	8.4	11.67	2.43	- 2.5

3.3 OBSERVATIONS

We want the observations to give information of the CLV for the intensity fluctuations in the spectral lines and nearby continua.

For each given spectral line the individual observations were carried out in the steps:

1) The image of the heliocentric position for which we wanted to observe in the line center was positioned on the slit.
2) The spectral line was scanned with channel 1 (in steps of 0.28-0.35 pm) with an entrance aperture of 1.5x170 arc.sec. in order to determine the average line profile at that heliocentric position. The widths of the exit slits were equivalent of 3pm and 20pm for channel 1 and 2, respectively. Channel 1 was thereafter positioned with an accuracy of 0.3pm at the center of the average profile. Channel 2 was manually placed in a nearby redwards continuum.

3) The entrance aperture was limited to 1.4 arc.sec. square. The image of the Sun was scanned in the east-west direction with a sampling interval of 35 *ms* (equivalent of 0.4 arc.sec. on the Sun) by letting the image drift across the slit.

For each line center position and spectral line 10-30 scans were observed. The data from each scan was divided into intervals of 5 degrees in heliocentric angle. Within these intervals the data were corrected for limb-darkening and large scale intensity structures by a least squares fitting of a third order polynomial. The r.m.s. intensity fluctuations ($\Delta I_{r.m.s.}$) were calculated within each interval. Figure 4 gives the CLV of the intensity fluctuations for the scans shown in Figure 2. The general trend of the CLV in the line (upper curve) should be compared with the hypothetical example in Figure 3.

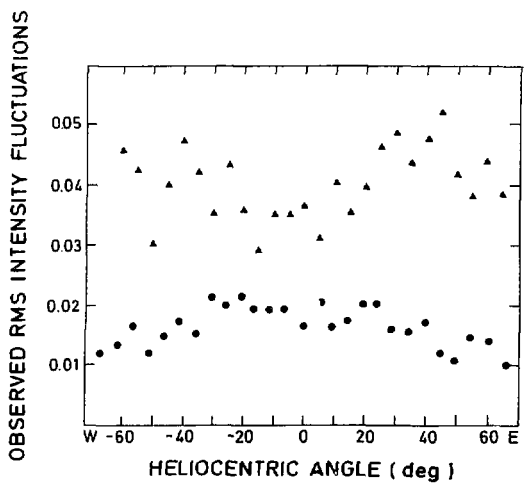

Fig.4. *The observed CLV of* $\Delta I_{r.m.s.}$ *of the scans shown in Figure 2. The values are calculated over intervals of 5 degrees in heliocentric angle. Triangles and dots indicate the results for the line and the continuum observations, respectively.*

A total of 165 scans were observed on 6 days between 6 August 1979 and 8 July 1980. 91 scans were found to have $\Delta I_{r.m.s.}$ in solar center continuum

larger than 1.5% and therefore included in the further study. For each scan the effect of different scan angles with respect to the solar equator was taken into account. Scans of the same lines and disc positions were averaged. Figures 5 and 6 show the average observed values for the lines 656.9 and 643.2 nm as dots.

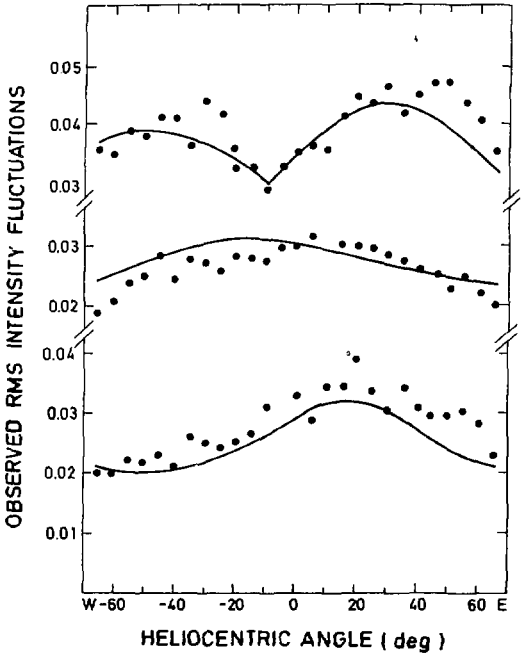

Fig.5. The average observed CLV of $\Delta I_{r.m.s.}$ observed in the FeI 656.9 nm line, shown as dots, is compared with the best fit of theoretical calculated values shown as the full drawn lines. The upper section shows the results for the scans observed in line center at solar disc center. The middle and lower section shows the results for scans observed with line centers at heliocentric angles of 30 degrees east and west, respectively.

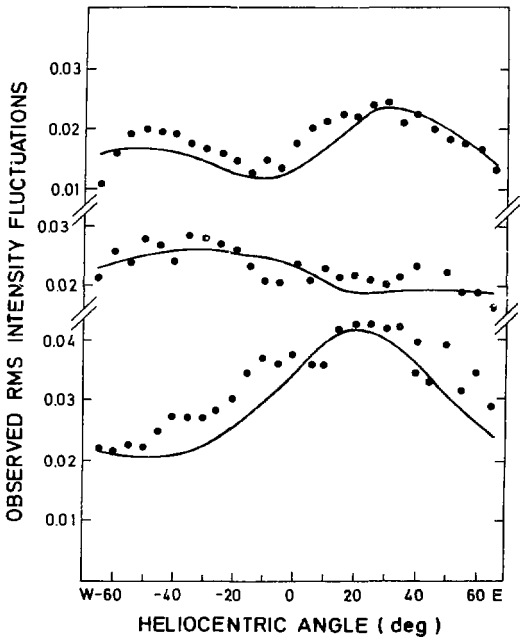

Fig.6. As for Figure 5, but observed in the Fe II 643.2 nm line and at 45 degrees heliocentric angle east and west, respectively.

3.4 PARAMETERS FOR THE VELOCITY MODEL

With the present method the velocity parameters are determined by comparing the theoretically calculated CLV of the intensity fluctuations with the observed (shown in Figures 5 and 6). To do the theoretical calculations it is necessary to make assumptions about several of the parameters entering into Equations 2 to 9.

Using the parameters derived from the average line profile calculations, LTE line profiles were calculated for each of the two components of the atmosphere presented by Nelson (1978). For each line and heliocentric angle the macro-turbulence was set equal to zero, whereas a wide range of micro-turbulence values were adopted. All calculations were done using Gaussian line profiles. From these calculations a grid of parameters for each line were chosen such that the average profile defined by equation 2 had an equivalent width within 5% of the value listed in Table I.

The continuum area ratio is fairly well determined, R=1.11±0.03 (Wittmann 1979, Andersen 1981). The true continuum contrast ratio A is assumed to be 0.80±0.05 (Wittmann 1979). Entering these parameters into equations 1-9, only the velocities and the spatial degradation parameter have to be determined.

For each scan the value of S needed to reduce the continuum intensity fluctuations, derived from the true contrast A_t to the observed fluctuations is found from equation 8. In our observations the values of S varied from 0.73 to 0.97, only values better than 0.9 were used. We note that the value for S in the very high resolution observations of BLT was 0.62.

The mathematical formulation used here (equations 2-9) assumes that all the observed intensity flutuations are caused by spatial fluctuations in a highly correlated velocity/intensity fields as described in Figure 3. This we know is not true. Superposed on granular velocities there are fluctuations caused by instrumental noise, changes in atmospheric transperancy and the solar intensity fluctuations caused by uncorrelated velocity/intensity fields.

The observed points are given as average values over several days. Since the effects mentioned above are spatially uncorrelated over this long time intervals they will contribute as a "noise" in the CLV of the fluctuations independent of the heliocentric angle. Because of the random nature of this "noise" in the average observed CLV of the intensity fluctuations, we can write for the observed intensity fluctuation as function of heliocentric angle,

$$\Delta I^2_{obs}(\theta) = \Delta I^2(\theta) + \Delta I^2_{noise} \qquad (10)$$

Here ΔI and ΔI_{noise} are the fluctuations from the granular field and all other contributions, respectively. From the equations 2 to 9 we find that the possible minimum values of ΔI is close to zero as demonstrated in Figures 1 and 3. Using Eq. 10 we find ΔI_{noise} which is equal to the minimum observed intensity fluctuation value ΔI_{obs}, confer Figures 4 to 6.

The line of sight velocity has contributions from both the horizontal and vertical components of the granular velocity field. In order to include both velocity directions in the model calculations it is necessary to make assumptions regarding the geometrical configuration of the velocity field. The method itself is independent of the choice of model. The complexity of the model should, however, be determined after taking into account the quality of the data. For simplicity we assume that the vertical components cause all the observed line shifts, whereas the horizontal components are responsible for the broadening of the lines. This simplified model is partly justified by the fact that the horizontal velocities change sign on smaller geometrical scales than the vertical velocity. Furthermore since only observations with heliocentric angle θ smaller then 60 degrees are used the vertical velocity will be the main contributor to the line of sight velocity.

The relative CLV of the line parameters are assumed to be equal in granules and in intergranular areas. The size is determined from the CLV of the average line profile.

An attempt was made to use the sinusoidal model of the velocity field proposed by Beckers and Nelson (1978). It was found that this and other detailed models introduced to many free parameters for our observational data. It is probable that for observations with higher angular resolution it is possible to determine the velocity model in greater detail. Higher accuracy could also be achieved by performing more detailed line profile calculations like those done by Nordlund (1980) and/or rejecting the computational convenient assumption of LTE.

3.5 GRANULAR VELOCITY RESULTS

The comparison between calculated and observed values of the intensity fluctuations was carried out as follows. The CLV of ΔI_{obs} was displayed on a graphical computer terminal. Interactively values for the vertical velocity differences and the horizontal velocity broadening were chosen. Using equations 1-10 the theoretical CLV was calculated and compared with the observed value. The deviations were calculated and stored. Successive velocity values were chosen in order to find the least deviation.

For all the lines except Fe I 557.6 nm it was possible to find unique combinations of vertical and horizontal velocities that reproduced the observed CLV of ΔI. The line parameters and velocities are given for each line and observed line center position in Table II. The theoretical CLV for two of the lines are shown in Figures 5 and 6.

Table II. Granular Line and Velocity Parameters.

Line (nm)	Line center observed at	Line parameters at disc center				Velocities (km/s)		Uncertainty in velocity
		B_q	B_l	$FWHM_q$	$FWHM_l$	V_{ver}	V_{hor}	
643.2	45 E	0.48	0.56	7.5	7.7	2.5	1.0	±0.5
	45 W					3.9	2.0	0.6
	0					2.6	1.0	0.4
643.2	45 E	0.45	0.49	8.0	7.7	3.0	1.5	0.4
	45 W					4.0	2.5	0.6
	0					3.2	1.4	0.5
656.9	30 E	0.10	0.10	11.0	9.9	2.0	1.2	0.5
	30 W					2.7	1.5	0.5
	0					2.2	1.0	0.4
659.3	45 E	0.21	0.21	12.0	10.2	0.4	0.5	0.3
	45 W					0.5	0.5	0.4
	10 E					0.4	0.5	0.3

The fitting of the theoretical curves to the observed ones can be done with an uncertainty in the velocities of 0.1-0.2 km/s. In addition the uncertainty caused by several possible combination of line parameters, the uncertainty in the continuum contrast and the uncertainty in the choice of the intensity model (equations 9 a,b) will introduce errors of 0.2-0.4, 0.18-0.25 and 0.1-0.15 km/s, respectively.

The variation in the velocity for different observational position of the line center is probably caused by the crude velocity model and the approximation done by assuming that the individual lines orginate at a level with constant velocity.

Keil (1980c) has discussed the effects of using this type of approximations when the velocity gradient with height is high. He found that the calculation of the velocity gradient directly in the line transfer function could change the velocity gradient nearly with a factor two as compared with the response function calculation.

From the fact that we are not able to reproduce the CLV of the intensity fluctuations in 557.6 nm, we conclude that there is little or no correlation between velocity and intensity at the heigths where central parts of this line is formed.

The height of formation for each line is a function of heliocentric angle, line parameters, velocity field and position in the line. The height of formation will increase with increasing heliocentric angle and decrease with increasing wavelength separation to the line center. For lines ob- increasing wavelength separation to the line center. For lines observed in line center at disc center the effect of observing higher regions in the atmosphere at increasing angles is partly compensated by wavelength shifts into the line wings caused by solar rotation.

In Figure 7 we have combined the calculated heights of line formation with the velocity results. The velocity differences in Table II have been transformed into r.m.s. velocities assuming a step function geometry of the velocity field (confer Eq. 9). We find that the velocities seem to decrease linearly to zero at approximately 200 km above $\tau_{500} = 1$. This is in accordance with the results of Keil (1980c) which are indicated with the dashed line in Figure 8. The linear equations derived for the velocities are (in km/s):

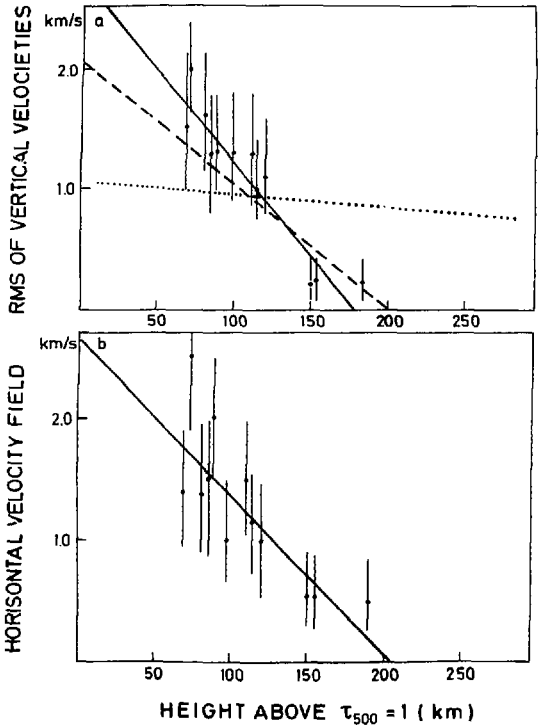

Fig.7. a) The r.m.s. of the vertical velocities, as function of height in the solar photosphere, are shown as dots with calculated uncertainties as vertical bars. The best linear fit to the points is given by the solid line. The height values were calculated from the response functions (Beckers and Milkey 1975). The dotted and dashed line show the results of Durrant et al. (1980c) respectively. b) As for a), but for the horizontal velocity field.

$$\Delta v_{r.m.s.} = 2.77 - 0.015 \cdot h(km),$$

$$\Delta v_{hor} = 2.66 - 0.013 \cdot h(km)$$

The results from Durrant et.al. (1979) indicate a much smaller velocity gradient with height as shown with the dotted line in Figure 7. They use, as do Keil (1980a,b), the method of directly measuring the Doppler shift of the spectral lines.

4. Discussion

Discussing the results presented in Figure 7 and equation 11 it must be emphasized that our method only measures the part of the velocity fluctuations where intensity and velocity are highly correlated. If this correlation decreases with height our results give an upper lim : for the true velocity gradient with height.

The measurement of this local correlation is difficult and uncertain. Some indirect information is obtained by determining the spatial correlation between elements observed in continuum and different parts of spectral lines. These measurements are influenced by the relatively short lifetime of the granules. Altrock and Musman (1976) find that the correlation disappears at a height of approximately 110 km above $\tau_{500} = 1$, Canfield and Mehltretter (1973) find a disappearing correlation at a height of 160 km. We have measured this correlation and the results are presented in Figure 8. When we exclude elements clearly larger that granules (>6") we find that the correlation disappears at approximately 190 km above $\tau_{500} = 1$.

The theoretical calculations of Nordlund (1980) show a correlation between local intensity- and velocity fluctuations that disappears at a height of approximately 100 km. The asymmetries observed in lines formed at greater heights indicate, however, that some correlation exists.

The equation of continuity imposes restrictions on how steep both the horizontal and vertical velocity gradients with height are allowed to be. We can write the equation of continuity as

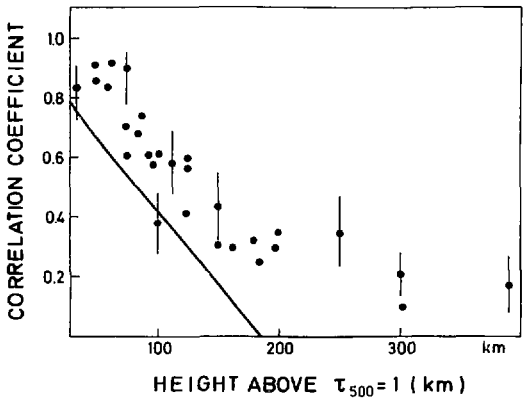

Fig.8. The cross correlation coefficient between intensity fluctuations (observed in 5 degree intervals) in spectral lines and in continuum as function of height in the solar photosphere. The full drawn line represents the best linear fit to the correlation values calculated when all structures larger than 6 arc.sec. are removed from the data.

$$\int_{z_o}^{z_1} \frac{\partial\ (\rho V_v)}{\partial\ z}\ dz = -\ 2 \int_{z_o}^{z_1} \frac{\partial (\rho\ V_h)}{\partial\ x} \cdot dz \qquad (13)$$

Here ρ is the density and z is the height parameter. The vertical and horizontal velocities are designated V_v and V_h respectively. Here we have assumed that the horizontal velocity field can be decomposed into two equal components. The typical values of the density scale height of 100-150 km and a horizontal scale of 500-1000 km give the observational constraints for the velocity gradients in equation 13. Entering these values and the observed vertical velocity gradient from equation 11 into equation 13 we find that the observed horizontal velocity gradient with height is too steep by a factor 2-3. This should indicate that our velocity gradients give an upper limit to the true value. This is probably caused by the decreasing correlation between velocity and local intensity with height. If we assume that the observed lower velocities in the line Fe I 659.3 nm is

caused by this decrease in correlation, then our observations would imply a velocity gradient closer to that of Durrant et al. (1979).

More observations are necessary in order to determine a reliable velocity gradient. These observations should include a larger number of lines with a large spread in heights of line formation. Our observational results for the lower photosphere (< 100 km) should, however, be reliable as the local intensity/velocity correlation is large there.

It should be noted that the line profiles in the granules are broader in the granules than in the intergranular areas (Table II). This is in clear contradiction to the results of Altrock and Musman (1976). Our results indicate a larger "microturbulence" in the granules than assumed earlier.

5. Conclusion

We have presented a new method for the measurement of granular velocities. This method has, as all other methods, its clear advantages and limitations. But since the limitations are not identical it can serve as a valuable supplement to the other methods. The advantages of our method can be summarized as:

1) It is less influenced by angular smearing. This is indicated by equal results under widely differing observing conditions.
2) It is statistically reliable as it employs a large number of granules.
3) No sophisticated equipment is needed for the observations and the data reductions are uncomplicated.

The limitations are:

1) The method measures only the highly correlated part of the velocity/intensity field.
2) Assumptions have to be made about the velocity and intensity fields.
3) It requires a large number of observations to reduce the effect of non-correlated velocity/intensity fluctuations.

Acknowledgement

The author wishes to express his sincere thanks to Dr. P.Maltby. Without his continous interest and pressure this paper would not have been written.

References:

Altrock, R.C. and Musman, S.: 1976, Astrophys.J. 203, 533.

Altrock, R.C., November, L.J., Simon, C.W., Milkey, R.W. and Worden, S.P.: 1975, Solar Phys. 43, 33.

Andersen, B.N.: 1979, Institute of Theoretical Astrophysics, Internal Report No. 9.

Andersen, B.N.: 1981, Thesis, University of Oslo (Unpublished).

Andersen, B.N., Engvold, O. and Pettersen, B.R.: 1977, Institute of Theoretical Astrophysics, University of Oslo, Report No. 50.

Baschek, B.: 1963, Z.Astrophys. 56, 282.

Beckers, J.M.: 1968, Solar Phys. 3, 258.

Beckers, J.M. and Milkey, R.W.: 1975, Solar Phys. 43, 289.

Beckers, J.M. and Nelson, G.D.: 1978, Solar Phys. 58, 243.

Brahde, R.: 1967, Institute of Theoretical Astrophysics, University of Oslo. Report No. 23.

Brahde, R.: 1974, Institute of Theoretical Astrophysics, University of Oslo. Report No. 41.

Brandt, P.N. and Schröter, E.H.: 1982, Solar Phys. 79, 3.

Bray, R.J., Loughhead, R.E. and Tappere, E.J.: 1976, Solar Phys. 49, 3.

Canfield, R.C. and Mehltretter, J.B.: 1973, Solar Phys. 33, 33.

Durrant, C.J., Mattig, W., Nesis, A., Reiss, G. and Schmidt, W.: 1979, Solar Phys. 61, 251.

Gingerich, O., Noyes, R.W. and Kalkofen, W.: 1971, Solar Phys. 18, 347.

Gray, D.F.: 1976, The Observation and Analysis of Stellar Photosphere. Wiley & Sons, New York.

Holweger, H. and Müller, E.A.: 1974, Solar Phys. 39, 19.

Howard, R. and Harvey, J.: 1970, Solar Phys. 12, 23.

Keil, S.L.: 1980 a, Astrophys.J. 237, 1024.

Keil, S.L.: 1980 b, Astrophys.J. 237, 1035.

Keil, S.L.: 1980 c, Astron.Astrophys. 82, 144.

Leighton, B.J., Noyes, R.W. and Simon, G.W.: 1962, Astrophys.J. 135, 474.

Marstad, N.: 1981, Institute of Theoretical Astrophysics, Internal Report No. 16.

May, M., Richter, J. and Nickelman, J.: 1974, Astr.Astrophys.Suppl. 18, 405.

Moore, C.E., Minnaert, M. and Houtgast, J.: 1966, Nat.Bur.Std. U.S. Monograph No. 61.

Nelson, G.D.: 1978, Solar Phys. 60, 5.

Nordlund, Å.: 1980, Stellar Turbulence. Lecture Notes in Physics 114. Ed. Gray, D.F. and Linsky, J.L.

Scherrer, P.H., Wilcox, J.M. and Svalgaard, L.: 1980, Astrophys.5. 241, 811.

Schröter, E.H., Wöhl, H., Soltan, O. and Vazquez, M.: 1978, Solar Phys. 4, 181.

Wittmann, A. and Mehltretter, J.P.: 1977, Astron.Astrophys. 61, 75.

Wittmann, A.: 1979, Small Scale Moitions on the Sun. Mitt.Kiepenheuer-Institut No. 179.

Wittmann, A.: 1981, Astron.Astrophys. 99, 90.

Manuscript received
December 14th. 1983.

INSTITUTE OF THEORETICAL ASTROPHYSICS
UNIVERSITY OF OSLO
P.O. BOX 1029, BLINDERN, OSLO 3, NORWAY

ISSN 0078-6780

Reports:

No. 35 (1972) *Øivind Hauge:* Isotopic Composition of some Metals in the Sun.

No. 36 (1972) *Lars Staveland:* Correction of Solar Intensity Measurements for Stray Light.

No. 37 (1972) *Hallvard Sørli and Oddbjørn Engvold:* A Comment on Contribution Functions.

No. 38 (1973) *Truls Lynne Hansen:* Comparison of Solar Seeing and Air Temperature Fluctuations at Oslo Solar Observatory.

No. 39 (1974) *O. Engvold and Ø. Hauge:* Elemental Abundances, Isotope Ratios and Molecular Compunds in the Solar Atmosphere.

No. 40 (1974) *O. Engvold, T. Kozar and B. Rompolt:* Motions in a Prominence of April 17, 1972.

No. 41 (1974) *Rolf Brahde:* Stray Light in Solar Observations.

No. 42 (1974) *Fritz Albregtsen* and *Truls Hansen:* The Theoretical Instrumental Profile of the Combination Telescope-Pinhole Photometer and its Effect upon Observations of Umbra Intensities.

No. 43 (1975) *Per Juell* and *Lars Staveland:* Correction of an Irregular Sunspot or Facula for Stray Light.

No. 44 (1975) *Bjørn M. Rustad:* The K and H Ca II Line Emission Ratio in Prominences.

No. 45 (1976) *Øyvind Iversen:* The Isotopic Abundance Ratio $^{12}C/^{13}C$ in the Solar Atmosphere Determined from CH-lines in the Photospheric Spectrum.

No. 46 (1976) *Bjørn Ragnvald Pettersen:* Catalogue of Flare Star Data.

No. 47 (1976) *Oddbjørn Engvold* and *Eberhart Jensen:* Stationary Flow in Magnetic Tubes of Force.

No. 48 (1977) *Øystein Elgarøy:* Solar Radio Noise Registrations at the Oslo Solar Observatory, 1965-74.

No. 49 (1977) *Ø. Hauge and O. Engvold:* Compilation of Solar Abundance Data.

No. 50 (1977) *B.N. Andersen, O. Engvold* and *B.R. Pettersen:* An Umbral Spectrum λλ 6812 - 6898 A.

No. 51 (1979) *Fritz Albregtsen:* A Four-Channel Infrared Pinhole Photometer for Solar Intensity Observations.

No. 52 (1981) *Truls S. Ringnes:* The Eighty Year Period in Short-Lived Sunspots.

No. 53 (1982) *Øystein Elgarøy:* Intermediate Drift Bursts.

No. 54 (1982) *Øystein Elgarøy* and *Øivind Hauge:* Solar Radio Noise Registrations at the Oslo Solar Observatory, 1975–81 and Comments on the whole Series of Measurements 1954–81.

No. 55 (1983) *O. Engvold* and *N. C. Marstad:* Solar Center-limb Variation of the Ca II K Line and the Wilson–Bappu Effect

No. 56 (1983) *H. Wöhl, O. Engvold and J.W. Brault:* Absortion Lines of FeH in a Sunspot Spectrum.

No. 57 (1983) *Ø. Elgarøy, C. Mercier, A. Tlamicha and P. Zlobec (eds):* Noise Storm Coordinated Observations. May 16–24, 81.

No. 58 (1983) *O. Kjeldseth Moe:* Astronomy From Space – Past and Future.

No. 59 (1983) Papers presented at Nordic Astronomy Meeting in Oslo. August 15–16, 1983.

No. 60 (1983) Papers presented at Nordic Astronomy Meeting in Oslo. August 17, 1983. Discussions on Nordic Optical Telescope.

No. 61 (1984) *Bo Nyborg Andersen:* A new Method for Measurement of Granular Velocities